  Bull. Chem. Soc. Jpn., 60, 3093—3097 (1987)

Metal Colloids Produced by Means of Gas Evaporation Technique. IV. Size Distribution of Small Mg and In Particles

Keisaku KIMURA
Instrument Center, Institute for Molecular Science, Myodaiji, Okazaki 444
(Received February 4, 1987)

Ultrafine metal particles with different sizes have been obtained by several preparation methods. The smallest Mg particles (the average diameter D_m of about 2 nm) were obtained by the matrix isolation method in He and the largest (D_m, 100 nm) by the conventional gas evaporation method in Ar. By changing the pressure and the kind of gas, particles with an intermediate diameter have been obtained. The size distribution of small In particles was discussed.

There are many reports on the preparation of fine metal particles with the diameter of less than 1 μm by the evaporation of metals in an inert gas.[1-5] However, it is not easy to obtain particles with the diameter of less than 10 nm by the conventional gas evaporation method, because particles become larger by coalescence when they contact with each other on the walls of preparation chamber. To prevent particles from contacting, a liquid is used for intervening between particles. Two approaches have been proposed. Yatsuya et al. reported the VEROS (vacuum evaporation on running oil substrate) method, in which a metal is evaporated in vacuum onto surface of running oil.[6-8] This method yields particles with a size of 3 nm, although there are severe restrictions on the selection of oil. The matrix isolation method combining the gas evaporation technique was also used by several researchers.[9-11] Furthermore, the gas flow-solution trap method and the gas flow-cold trap method were developed in the previous studies by the present author using organic liquids as substrate.[11,12] The particle diameter at the maximum distribution reached the range of 1 nm. Several kinds of well dispersed ultrafine metal particles were obtained such as Ni, Ag, Cu, Au, Sb, and Al by Wada[9] and Ag, Au, Cu, In, Al, Ca, Sn, and Pb by the present author.[11] The reaction of metal particles with liquids and the change in particle diameter due to the reaction were examined in a previous work.[12]

A wide difference of particle diameter between the conventional gas evaporation method (several tens nm) and the liquid substrate method (several nm) suggests difference in particle growth mechanism. The mechanism of nucleation growth from gaseous atoms was studied by analyzing size distribution of the particles produced. As is usually seen in many physical processes, the normal distribution results from a random process. Granqvist[13,14] proposed the log-normal distribution for the metal particles produced by the gas evaporation method. His proposal was confirmed for extremely small particles prepared by the VEROS method[15] irrespective of large difference in particle diameter between two methods. Since no study was performed on the nucleation mechanism of small particles produced by the matrix isolation method, the gas flow-solution trap method, and the gas flow-cold trap method, this paper describes the size distribution by differnt preparation methods in the case of Mg particles in tetrahydrofuran (THF) and In particles in acetone.

Experimental

Small metal particles were prepared by the matrix isolation method, the gas flow-solution trap method, and the gas flow-cold trap method similarly as described in the previous paper.[11] Several kinds of gas atmosphere were examined: He and Ar for the matrix isolation method, and a He/Ar mixture as well for the gas flow method were used. The metals used were 99.999% In, 99.99% Mg, and 99.5% Au. Acetone was purified with CaH_2 and THF was distilled from its Na-benzophenone solution. The size distribution of particles was determined by electron microscopy. A colloidal solution was dropped on a Cu mesh coated with evaporated carbon film of 10 nm in thickness. Hitachi H-500H electron microscope of the Laboratory of Electron Microscopy, the National Institute for Physiological Sciences at Okazaki was used with a 100 kV high resolution mode. The histograms of size distribution were obtained by an Image Analyser, Kontron IBAS-1, of the Center for Analytical Instrument, the National Institute for Basic Biology at Okazaki.

Results and Discussion

Size Distribution of Mg Particles. Figure 1 shows micrographs of Mg particles produced by different methods. The finest particles in Fig. 1a were prepared by the matrix isolation method in He gas atmosphere. Figure 1b shows Mg particles prepared by the same method but in Ar atmosphere. The largest particles in Fig. 1c[16] were obtained by the conventional gas evaporation method in Ar atmosphere, in which hexagonal crystal habit characteristic of hcp structure is seen. The size distributions curves f(d) in Fig. 2 were obtained from Figs. 1a, 1b, and 1c, respectively. It is evident that the average diameter widely varies from 2 to 100 nm with the preparation

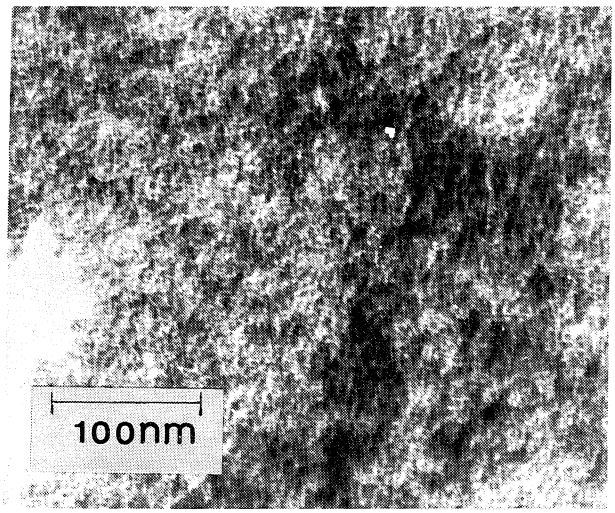

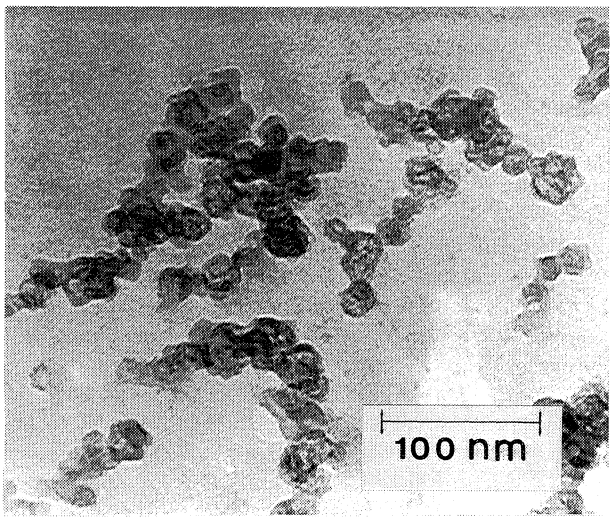

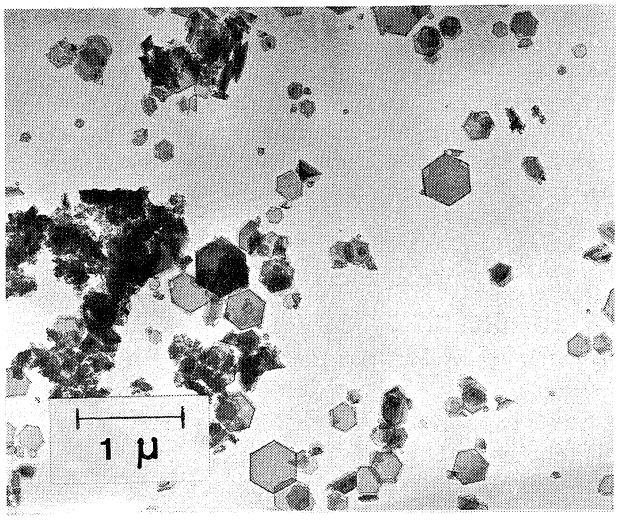

Fig. 1. Electron microscope images of Mg small particles of different sizes.
a) Mg/THF produced by the matrix isolation method in He gas of 1.3 kPa. b) Mg/THF produced by the matrix isolation method in Ar gas of 300 Pa. c) Produced by the conventional gas evaporation method in Ar gas of 4 kPa.[16]

method and conditions. The number of atoms in a single particle accordingly varies from 10^2 to 10^7. This result differs from that of giant clusters produced by the supersonic nozzle beam method, in which the size distribution is a monotonously decreasing function of the size modulated by small cusps at the position of magic numbers.[17,18] It is also noteworthy that the half-value width of distribution is a function of the average diameter. The smaller the particle diameter is, the narrower the width of distribution becomes. This tendency was also reported for Al particles produced in He gas.[19]

The effect of mass and pressure of inert gas on the particle size was reported by Wada on the conventional gas evaporation method.[20] The particle size increases in the order of He, Ar, and Xe. The size also increases with increasing ambient gas pressure. In this experiment, larger particles (Fig. 1b) were obtained in Ar than in He (Fig. 1a). The distribution in Fig. 1b (the diameter at the maximum distribution D_m of 19 nm) is close to that by the gas evaporation method in He (D_m, 21 nm). This shows that the gas evaporation method in a gas with small molecular weight yields the particles of size equivalent to that by the matrix isolation method in a gas with large molecular weight. It seems evident that the matrix isolation method is superior to the gas evaporation technique in order to obtain ultrafine particles when we expect the quantum size effect. For Mg metal, a particle of 2.1 nm (Fig. 1a) is composed of 210 atoms and, therefore, the average electron level spacing near the Fermi level is about 130 K, which is far above the normal cryogenic temperature.[21] Hence, it is easy to observe the quantum size effect for these particles.[22,23]

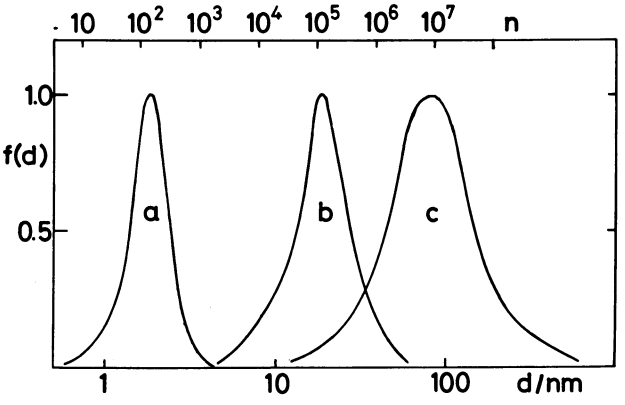

Fig. 2. Size distribution of Mg small particles produced by different method.
Curves, a, b, and c are from those in Fig. 1. The distribution maxima locate at the diameter (D_m) of 2.1 nm for a, 19 nm for b, and 100 nm for c. Numbers in the top abscissa are the number of Mg atoms in a particle whose diameter is designated in the bottom abscissa.

Analysis of Size Distribution of In Particles. Particle size distribution strongly depends on its growth process. Two main processes have been proposed:[24] One is the absorption growth process where particle nuclei grow up with absorption of metal atoms. This gives the normal distribution of particle size. Another is the coalescence growth process where particles grow up by collision of particle nuclei to give a log-normal size distribution. This distribution is derived from the assumption that the change in volume (mass) at each step is a random fraction of the volume after coalescence. The normalized distribution for logarithm of volume is given by

$$f_{LN}(v) = \frac{1}{\sqrt{2\pi}\ln\sigma_v}\exp\left\{-\frac{1}{2}\left[\frac{\ln(v/\bar{v})}{\ln\sigma_v}\right]^2\right\}, \quad (1)$$

where $\bar{v}$ is the mean volume and σ_v is the standard deviation of volume. The number of particles Δn per logarithmic volume interval is, therefore, given by $\Delta n = f_{LN}(v)\Delta(\ln v)\cdot n$. For a sphere particle, one obtains the so-called log-normal distribution function for particle diameter, d, as

$$f_{LN}(d) = \frac{1}{\sqrt{2\pi}\ln\sigma}\exp\left\{-\frac{1}{2}\left[\frac{\ln(d/\bar{d})}{\ln\sigma}\right]^2\right\}. \quad (2)$$

The fraction of the number of particles per diameter interval can be written as $\Delta n/n = f_{LN}(d)\cdot\Delta d/d$.[14] For the log-normal distribution, the mean diameter d is related to the peak diameter D_m as $\bar{d} = D_m\cdot\exp[\ln\sigma]^2$.

Figure 3 shows a typical size histogram of In particles produced by the gas flow-cold trap method in acetone. The best fit with the log-normal distribution is shown by a broken line in Fig. 3. The features of fitting are wholly good. Since it is difficult to achieve the best fit only from the appearance of fitting to the distribution curve, a better technique will be found with reference to graphical "normal-probability" and "log-probability" analyses as stated below. If the size distribution is a linear normal distribution, cumulation of the number of particles of a certain size follows the error function and plotting of the points on normal probability paper will give a straight line. Figure 4a shows the normal-probability plot of the sample shown in Fig. 3. It is clear that the size distribution does not fit with the normal distribution. On the other hand, the log-probability plot of the same sample gives a good straight line as shown in Fig. 4b, indicating that the size distribution of this sample is of a log-normal. The fitting was also checked by the χ^2-test with sample number 250 and the number of classes 29. The best fitting was obtained with σ of 2.13 and $\bar{d}$ of 20 nm and shown in Fig. 3 by a broken line. The significance level is over 75%

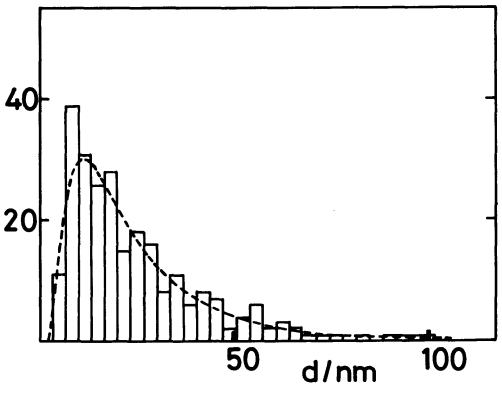

Fig. 3. Size histogram for In samll particles produced by the gas flow-cold trap method in acetone. The pressure of He+Ar mixed gas was 1.3 kPa. Broken line is a calculated curve from the log-normal distribution with fitted parameters σ=2.13 and $\bar{d}$=20 nm. The ordinate represents the number of particles at a given size interval.

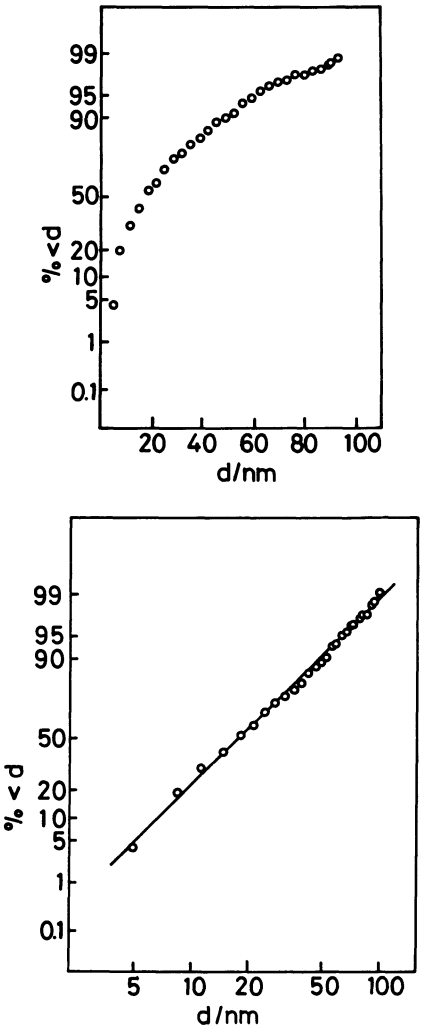

Fig. 4. a) Normal-probability plot and b) log-probability plot for In small particles. The ordinate stands the cumulative percent of particles with diameters smaller than d.

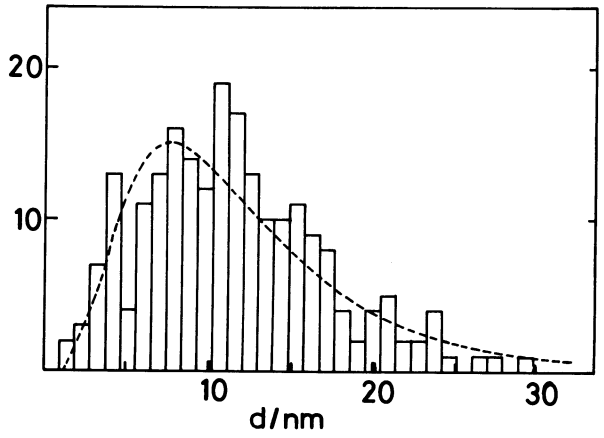

Fig. 5. Size histogram for In small particles produced by the matrix isolation method in acetone. The N_2 gas pressure was 1.3 kPa. Broken line is a calculated curve from the log-normal distribution with fitted parameters σ=1.8 and $\bar{d}$=10.8 nm. The ordinate represents the number of particles at a given size interval.

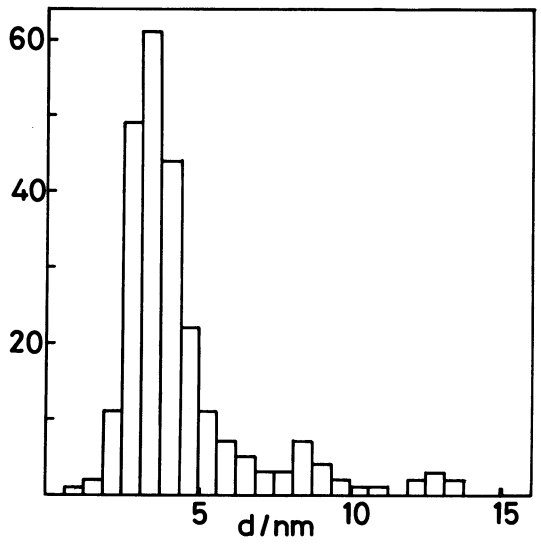

Fig. 6. Size histogram for In small particles produced by the gas flow-solution trap method in acetone.
The He gas pressure was 1.3 kPa. The peak diameter D_m=3 nm. No fitting was obtained for normal-probability and log-probability plots. The ordinate represents the number of particles at a given size interval.

showing the strong reliability of this fit, because the rejection level is normally set at 1 or 5%.

Figure 5 shows the size histogram of In particles produced by the matrix isolation method in acetone under N_2 atmosphere. The fitting of size distribution with the log-normal distribution was also checked by the χ^2-test with a significance level of 30%. This result seems to confirm that the log-normal distribution is applicable to this sample. The technique of the matrix isolation method is similar to that of the conventional gas evaporation method only except for the substrate of low temperature organic matrix.

Figure 6 shows the size histogram of small In particles produced by the gas flow-solution trap method in acetone under He atmosphere. In this preparation, the diameter of maximum distribution is about 3 nm. It was confirmed that the smallest particles are formed in low pressure He as in the case of Mg shown in Fig. 2. The histogram in Fig. 6 fits with neither the normal-distribution nor the log-normal distribution. The size distribution of Au particles in acetone produced by the same method (D_m=1.1 nm) fits with neither of two distribution curves. These distribution functions are derived on the assumption that the system is in thermodynamical equilibrium during particle growth. This is the case for a closed chamber atmosphere such as the conventional gas evaporation method and the matrix isolation method but not for the gas flow method, in which a constant flow of inert gas turbulates the nucleus growth process. The size distribution in Fig. 6, therefore, shows the distribution at the beginning of particle growth. Narrow size distribution of particles supports this assumption. Nevertheless, we need to know why the log-normal distribution is observed in the gas flow-cold trap method as shown in Fig. 3. In this method, the particles co-deposit with organic vapor on the walls of glass reaction vessel and are embedded in the matrix. The volume fraction of metal is so high in the matrix that particles tend to coagulate in the matrix. Large particles of 20 nm produced by the gas flow-cold trap method probably reflect the coagulation process, because the size of particles in a gas stream is believed to be of the order of 3 nm. It will be suggested that the size of small metal particles could be widely and easily changed from 2 to 100 nm in any suitable organic liquid, although only tetrahydrofuran and acetone were examined in the present study.

The author expresses his gratitude to Prof. Sanshiro Sako for presenting the photograph of Mg particles produced by the conventional gas evaporation method.

References

1) L. Harris, D. Jeffries, and B. M. Siegel, *J. Appl. Phys.*, **19**, 791 (1948).
2) K. Kimoto, Y. Kamiya, M. Nonoyama, and R. Uyeda, *Jpn. J. Appl. Phys.*, **2**, 702 (1963).
3) K. Kimoto and I. Nishida, *Jpn. J. Appl. Phys.*, **6**, 1047 (1967).
4) N. Wada, *Jpn. J. Appl. Phys.*, **7**, 1287 (1968).

5) S. Kasukabe, S. Yatsuya, and R. Uyeda, *Jpn. J. Appl. Phys.*, **13**, 1714 (1974).
6) S. Yatsuya, K. Mihama, and R. Uyeda, *Jpn. J. Appl. Phys.*, **13**, 749 (1974).
7) S. Yatsuya, T. Hayashi, H. Akoh, E. Nakamura, and A. Tasaki, *Jpn. J. Appl. Phys.*, **17**, 355 (1978).
8) S. Yatsuya, Y. Tsukasaki, K. Mihama, and R. Uyeda, *J. Cryst. Growth*, **45**, 490 (1978).
9) N. Wada, *J. Phys. (Paris)*, **C2**-219 (1977).
10) H. Abe, W. Schulze, and B. Tesche, *Chem. Phys.*, **47**, 95 (1980).
11) K. Kimura and S. Bandow, *Bull. Chem. Soc. Jpn.*, **56**, 3578 (1983).
12) K. Kimura, *Bull. Chem. Soc. Jpn.*, **57**, 1683 (1984).
13) C. G. Granqvist and R. A. Buhrman, *J. Appl. Phys.*, **47**(5), 2200 (1976).
14) C. G. Granqvist, *J. Phys. (Paris)*, **C2**-147 (1977).
15) K. Koide, S. Yatsuya, and I. Yoshimura, *Jpn. J. Appl. Phys.*, **19**(2), 367 (1980).
16) S. Sako and K. Kimura, *J. Phys. Soc. Jpn.*, **53**(4), 1495 (1984).
17) J. B. Hopkins, P. R. R. Langridge-Smith, M. D. Morse, and R. E. Smalley, *J. Chem. Phys.*, **78**, 1627 (1983).
18) D. M. Cox, D. J. Trevor, R. L. Whetten, E. A. Rohlfing, and A. Kaldor, *J. Chem. Phys.*, **84**, 4651 (1986); *idem, Phys. Rev. B.*, **32**, 7290 (1985).
19) S. Yatsuya, S. Kasukabe, and R. Uyeda, *Jpn. J. Appl. Phys.*, **12**, 1675 (1973).
20) N. Wada, *Jpn. J. Appl. Phys.*, **7**, 1287 (1968).
21) W. P. Halperin, *Rev. Mod. Phys.*, **58**(3), 533 (1986).
22) K. Kimura, S. Bandow, and S. Sako, *Surf. Sci.*, **156**, 883 (1985).
23) K. Kimura and S. Bandow, *Phys. Rev. Lett.*, **58**, 1359 (1987).
24) G-Hanne Comsa, *J. Phys. (Paris)*, **C2**-185 (1977).